

# Ultra-thin silver electrodes for high power density pulse batteries

Xianbo Jin, Juntao Lu<sup>\*</sup>, Yong Xia, Peifang Liu, Hua Tong

*School of Chemistry and Environmental Science, Wuhan University, Wuhan 430072, China*

Received 28 August 2000; received in revised form 08 November 2000; accepted 05 April 2001

## Abstract

Ultra-thin silver electrodes for high power density pulse batteries are prepared by anodic oxidation and cathodic reduction of thin silver foils in 0.1 mol/l HCl aqueous solution. The active layer thus formed has a porosity about 65%. The thickness of the active layer can be controlled by the charge passed in oxidation. Typically, silver foils 50  $\mu\text{m}$  thick are used as the raw material and finished in 80  $\mu\text{m}$  electrodes with nominal capacity 14 C/cm<sup>2</sup> on each side. These electrodes can be charged and discharged at very high rates (typically 10C charge and 10<sup>2</sup>C discharge) with about 90% utilization of the active material. Potential valleys, most possibly due to the resistive Ag<sub>2</sub>O, are observed on both steady-state and pulse discharges. To prevent the potential valleys, which are most annoying to pulse applications, charging is suggested to be confined within the low potential plateau region. © 2001 Elsevier Science B.V. All rights reserved.

*Keywords:* Silver electrodes; Zinc–silver batteries; Pulse batteries; Pulse discharge

## 1. Introduction

Despite of the advent of new battery systems of high performance such as lithium ion and metal hydride systems, zinc–silver oxide batteries are still the best in terms of power density [1]. The superiority in power density makes zinc–silver oxide system the top choice for applications where volume and weight are critical and high power output is required, such as the high power density pulse batteries.

Unlike the batteries for most of other applications, the pulse batteries do not need a high capacity but have to be able to discharge at a very high rate. For those batteries, power density instead of energy density is the top priority. To meet the requirement of high power density, the active material layer of the electrode should be very thin (microns to tens of microns depending on applications). For an ultra-thin electrode of this kind to be able to discharge at a very high rate (10<sup>2</sup>C), the active material must be porous and composed of highly dispersed particles. It is difficult to make such a thin layer on a large surface area with reasonable reproducibility if traditional methods are used, such as sintering or pressing of powder materials. Takeda and Hattori reported an optimized method to manufacture silver electrodes for high drain pulse batteries [2] for low power applications. This paper reports a new approach based on electrochemical formation and reduction of silver chloride

on a silver substrate to make ultra-thin silver electrodes for high power pulse batteries.

## 2. Experimental

### 2.1. Electrode preparation

A silver foil 50  $\mu\text{m}$  thick was used as the raw material for the ultra-thin silver electrode. The foil was cut into a rectangular 1.5 cm wide and 2 cm high with a strip of about 3 mm wide to serve as the electrical lead. Both sides of the foil were used as the working electrode surface and the effective apparent surface area was 6 cm<sup>2</sup>. After degreased in acetone and washed with distilled water, the electrode was etched in concentrated nitric acid for about 10 s and washed with distilled water again. Then the electrode was subjected to anodic treatment in 0.1 mol/l HCl at a constant current density. The counter electrodes were two silver foils of the same shape and size as the working electrode and placed on the two sides of the working electrode at equal distances. The three electrodes were fitted in a rectangular electrolytic bath with the cross-section of the electrolyte being the same as the working areas of the electrodes to ensure a uniform current distribution. This cell configuration was used throughout this work, including electrode preparation and electrochemical measurements. After a required charge had passed, the current direction was reversed to convert the chloride into porous metallic silver. The working electrode

<sup>\*</sup> Corresponding author. Tel.: +86-27-7647617; fax: +86-27-87647617.  
E-mail address: jtl@whu.edu.cn (J. Lu).

was withdrawn from HCl bath and, after washed with distilled water, transferred to 30% KOH for activation by charge–discharge cycling. The finally finished working electrode was in charged state. In most of the experiments described below, a porous layer about 20  $\mu\text{m}$  thick was formed on both sides of the electrode and the rest solid silver in the center of the foil served as the electrical collector and the mechanical support for the active layer.

## 2.2. Electrochemical measurements

During anodic formation of AgCl, the electrode potential was monitored against an Ag/AgCl reference electrode with a Luggin capillary and recorded on a  $Y-t$  recorder. For performance tests, the working electrode was discharged with either constant or pulse current in 30% KOH and the potential was recorded against the Zn electrode in the same solution. All discharge tests were carried out at 25°C. The double layer capacity was estimated according to the current of cyclic voltammetry in the potential region 0.30–0.35 V (versus Zn). Scanning electron microscope (Hitachi X-650) was used to examine the morphology of the electrode.

## 3. Results and discussion

### 3.1. Electrochemical formation of AgCl

It is well known that repetitive oxidation and reduction of a metal may lead to formation of a porous layer on the surface. However, it is not easy to produce a porous layer satisfying specific technical demands by using this principle. We had tried KOH, NaAc–HAc mixture, bromide solution and iodide solution, but none of them gave satisfactory results. In KOH solution, no sufficient amount of active material could be formed in several oxidation–reduction cycles. In NaAc–HAc solution, the AgAc crystals formed were too large for our purpose. Fortunately, we finally found HCl solution suitable. In this solution, a chloride layer of required thickness can be easily formed in a single process of oxidation and the AgCl layer thus formed can be readily reduced to a porous silver layer with fine structure and smooth macroscopic appearance. Bromide and iodide behave similar to chloride in forming salt with silver. However, AgBr and AgI are more photosensitive than AgCl and we have found that photo-decomposition of the salt has a deleterious effect on the performance of the electrode produced. The last but not the least, chloride is low in cost and environment friendly. Therefore, chloride system was chosen for the electrode preparation.

Fig. 1 shows the potential change with the charge passed for etched silver foils during anodic treatment in 0.1 mol/l HCl at different current densities. For the lowest current density used (0.2 mA/cm<sup>2</sup>), the potential change may be roughly divided into three stages (curve a in Fig. 1). In the first stage, potential increased with time approximately

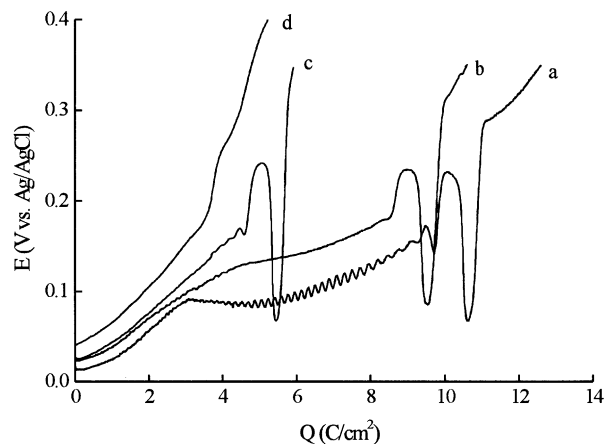


Fig. 1. Potential change during AgCl formation at different current densities (mA/cm<sup>2</sup>): (a) 0.2; (b) 0.3; (c) 0.5; (d) 1.0.

linearly till about 3 C/cm<sup>2</sup>. In the following stage, the increase of potential became slower with small amplitude vibrations which are thought to be caused by fine cracking of the existing AgCl layer. Above approximately 0.18 V versus Ag/AgCl, large amplitude potential vibrations were superimposed on an accelerated increase of potential and bubbles were observed on the electrode surface. For slightly higher current densities (curves b and c in Fig. 1), the situations were similar to curve a, but the second stage was shortened with increasing current density and the small amplitude vibrations were less visible. At the highest current density studied (curve d in Fig. 1), the second stage disappeared completely and neither small nor large amplitude vibration was found, perhaps indicating a mechanically stronger AgCl layer formed on the surface. The electrochemical formation mechanism of the silver chloride on a silver substrate in chloride-containing solutions has been discussed in a number of papers [3–5]. Katan reported that a compact AgCl layer of about 1.14 C/cm<sup>2</sup> was formed in the initial phase [6]. The first stage of curve a in Fig. 1 may correspond to the development of this kind of compact layer. The AgCl layer formed galvanostatically at high current densities (0.01–10 A/cm<sup>2</sup>) in concentrated KCl solutions (4–14 mol/l) has also been investigated [7], and large amplitude potential vibrations were reported to begin when the passed charge reached about 1 C/cm<sup>2</sup>. These literature reports are in qualitative agreement with our findings. Because violent gas evolution would eventually destroy the AgCl layer, potentials over 0.18 V should be avoided. Therefore, a lower current density should be adopted if a higher loading of AgCl is to be formed on the electrode surface. In this work, 0.2 mA/cm<sup>2</sup> was used as routine to prepare electrodes with an AgCl loading about 7 C/cm<sup>2</sup> which is equivalent to a nominal capacity of 14 C/cm<sup>2</sup> for AgO (assuming 100% utilization of the active material).

The anodic treatment in HCl should be conducted in a place without strong light (such as direct sun shining) or the AgCl coating would become dark and the performance of finally finished electrodes would be affected disadvantageously. A

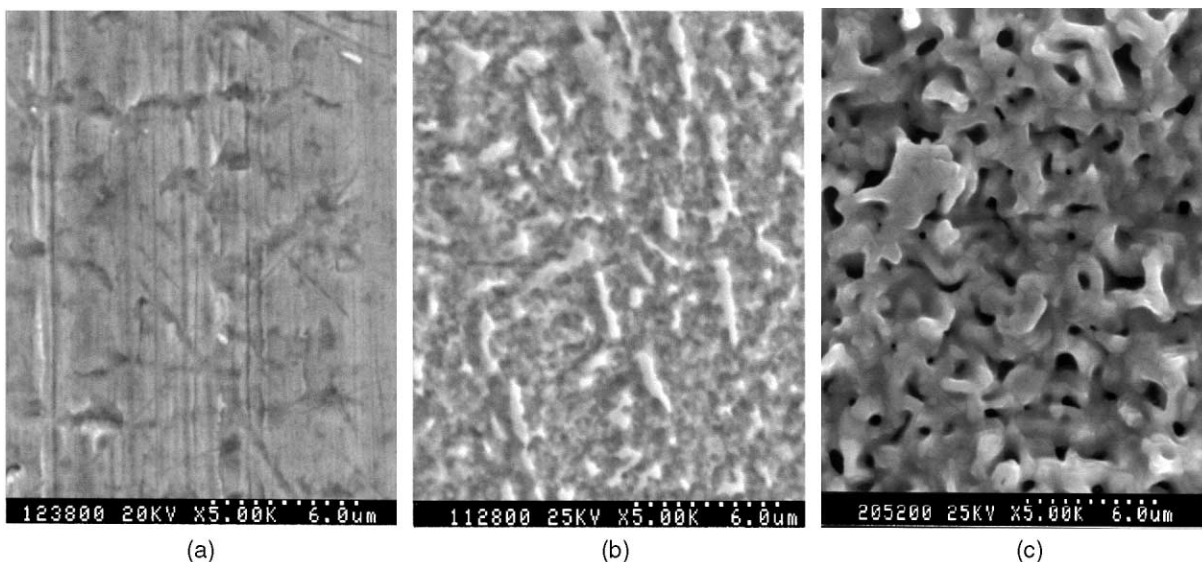


Fig. 2. SEM images of the silver electrode: (a) cleaned; (b) etched; (c) AgCl deposited ( $7.2 \text{ C/cm}^2$ ).

well prepared AgCl coating had a macroscopically smooth appearance in brownish color. The macroscopic uniformity is important for manufacturing large area electrode with good reproducibility. We have successfully produced electrodes of the size  $3 \text{ cm} \times 6 \text{ cm}$  and no sign of limitation was found for further enlargement. The thickness of the electrode was increased on chlorization. For example, a  $7.2 \text{ C/cm}^2$  AgCl coating had a thickness of  $21.7 \mu\text{m}$  compared with  $7.7 \mu\text{m}$  of the metallic silver consumed on formation of the chloride.

Fig. 2 shows the morphological changes of the electrode in the above mentioned processes. The original surface of the silver foil had irregular scratches (Fig. 2a). After etching, shallow pits were spread over the surface and the original scratches were no longer visible. The etching process provided a fresh and uniformly roughened surface which was

crucial for the reproducibility of electrode manufacturing. Fig. 2c shows the AgCl coating ( $7 \text{ C/cm}^2$  of charge) which exhibited complex morphological patterns ranging  $1\text{--}3 \mu\text{m}$  in size.

### 3.2. Converting AgCl into porous metallic Ag

The AgCl coating was reduced at a cathodic current density about  $0.2 \text{ mA/cm}^2$  till gas evolution in the same bath where AgCl had been formed. The electrode thickness was essentially not changed during reduction. For the above mentioned example, a 65% porosity can be deduced from the coating thickness and the charge passed in chlorization. The SEM observation of a reduced coating revealed networks composed of silver particles in different shapes and sizes (Fig. 3a).

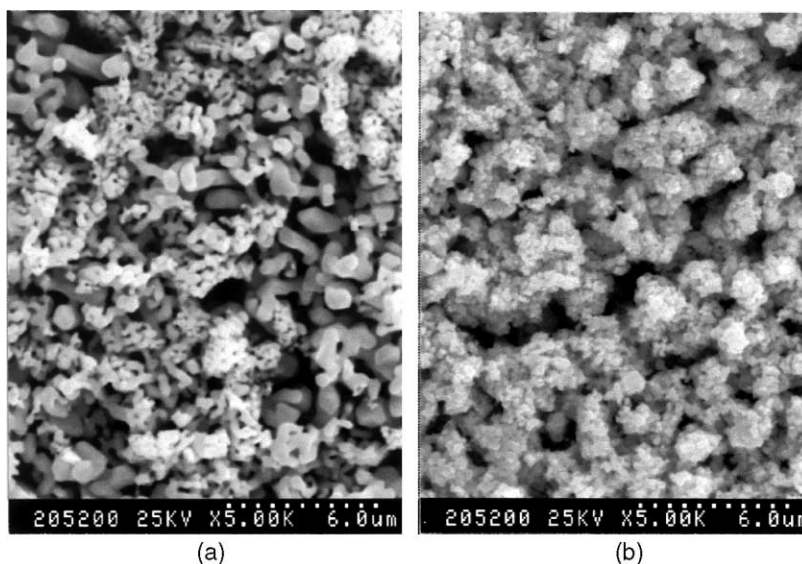


Fig. 3. SEM images of the porous silver layer before (a) and after (b) activation.

The AgCl structures on the top layer were mainly converted to fine spherical silver particles about 0.1–0.2  $\mu\text{m}$  in diameter while the underlying structures converted into banana-shaped cylinders with diameters around 1  $\mu\text{m}$ . Cyclic voltammetry of the reduced electrode in 30% KOH presented a double layer capacity 3.9  $\text{mF}/\text{cm}^2$ . As well known, the double capacities for electrochemical surface are about 40 and 20  $\mu\text{F}/\text{cm}^2$  for positively and negatively charged surfaces, respectively. Unfortunately, we failed to find reliable data for the zero charge potential of silver in 30% KOH. For a rough estimation of the electrochemical surface area, we took the average value 30  $\mu\text{F}/\text{cm}^2$  as the specific double layer capacity instead. Then the electrochemical surface area for 1  $\text{cm}^2$  apparent electrode area turned out to be 130  $\text{cm}^2$ . Assuming spherical shape, the average diameter of the silver particles was estimated to be 0.36  $\mu\text{m}$ , in reasonable agreement of SEM observation.

### 3.3. Electrochemical activation

The reduced porous silver electrode was transferred to 30% KOH for activation by charge and discharge cycling. After four cycles of 60  $\text{mA}/\text{cm}^2$  charge and 400  $\text{mA}/\text{cm}^2$  discharge, the apparent double layer capacity increased from 3.9 to 12.7  $\text{mF}/\text{cm}^2$ , implying a decrease of average particle diameter from about 0.36 to 0.11  $\mu\text{m}$ . The about three-fold decrease in particle size in the activation process proved to be significant to the electrode discharge performance. Fig. 3 compares the microstructures of the porous silver layer before and after activation. It is evident that activation improves effectively the dispersity of the active material. The finished silver electrode, in either charged or discharged state, was mechanically strong enough to perfectly survive the successive processes of battery manufacturing and vibrations possibly encountered in real applications.

### 3.4. Steady-state discharge

The ultra-thin silver electrode composed of fine particles allows high rate charge and discharge. Experiments showed that charge current densities ranging from 0.3 to 60  $\text{mA}/\text{cm}^2$  resulted in essentially the same discharge performance though the electrode charged at higher rates showed darker color than those charged at lower rates. In the following sections, the electrodes were routinely charged at 60  $\text{mA}/\text{cm}^2$  (ca. 15C rate).

The steady-state discharge curves shown in Fig. 4 were obtained immediately after charging the electrode to gas evolution. At lower discharge rates, two potential plateaus were clearly seen with the higher plateau shorter than the lower one. At the highest current density tested (1.5  $\text{A}/\text{cm}^2$ ) the higher plateau almost disappeared completely. The shortened higher plateau was already reported and discussed in literature in the early stage of development of silver oxide electrodes [8] and remains to be a topic of study. In this paper we do not intend to go further with the mechanism discus-

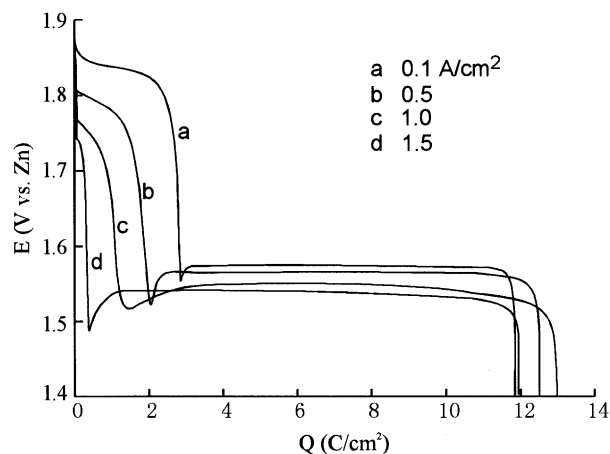


Fig. 4. Steady-state discharge immediately after charging to gas evolution. Discharge temperature 25°C.

sions and will focus on the electrode performance instead. It is seen in Fig. 4 that the discharge capacities of the ultra-thin silver electrode at 0.1 and 1.5  $\text{A}/\text{cm}^2$  were very close to each other while the capacities at 0.5 and 1.0  $\text{A}/\text{cm}^2$  were even marginally higher. The unusual non-monotonic dependence of the capacity on current density was also observed in other measurements and the reason might be related to the special structure of the ultra-thin electrodes but the details remain for further study. However, taking the nominal capacity to be 14  $\text{C}/\text{cm}^2$  (according to 7  $\text{C}/\text{cm}^2$  AgCl), the utilization of active material reached  $90 \pm 5\%$  which should be considered rather high in view of the high discharge rates (26–386C).

Between the high and low plateaus, there was a potential valley as usually observed with other kind of silver oxide electrodes. If the fully charged (up to oxygen evolution) electrode had been stored for a few hours or more either in the solution or in dry state, an additional deep potential valley appeared at the very beginning of discharge for all the discharge current densities studied in this work. The potential valley during discharge and the potential peak during charge have long been reported and are attributed by many researchers to the high resistivity of  $\text{Ag}_2\text{O}$  [9–11], but different explanations are also seen in [8,12]. Fig. 5 shows the discharge curves obtained at the same current densities as in Fig. 4 for an electrode charged only 4  $\text{C}/\text{cm}^2$  (about 60% of the electricity for  $\text{Ag}_2\text{O}$  formation). There was no potential valley and the polarization was slightly smaller than that in Fig. 4. A comparison of Figs. 4 and 5 provides a support to the assumption that a compact  $\text{Ag}_2\text{O}$  layer over the particles or the silver substrate may be responsible for the potential valley.

High power pulse batteries are not to be used as secondary batteries in typical applications. However, good cycling performance is desirable in some cases. Fig. 6 shows that there were only marginal changes in capacity during the first 20 cycles under very hard conditions, i.e. being discharged at 103C rate down to 1.45 V (versus Zn) and charged at 15.4C

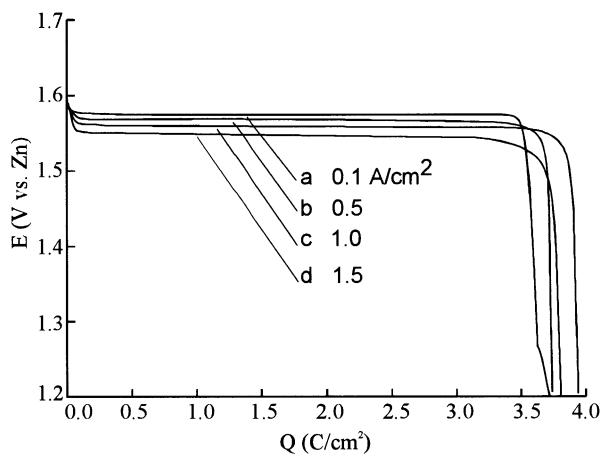


Fig. 5. Steady-state discharge immediately after charging to  $4 \text{ C/cm}^2$ . Discharge temperature  $25^\circ\text{C}$ .

rate. Based on the value  $14 \text{ C/cm}^2$  for the nominal capacity, the utilization efficiency of active material was about 88%.

### 3.5. Pulse discharge

Like the situation in steady-state discharge, the pulse discharge performance of the ultra-thin silver electrode depended on the state of charge and history. For the electrodes discharged immediately after being charged to gas evolution, the representative results for the first five pulses in the high and low potential plateaus are given in Fig. 7. In the high plateau region (curve a in Fig. 7), the potential responses to current pulses looked normal for a porous electrode and the polarization during pulses was about 50 mV. When the discharge potential went just down to the low plateau region, however, a potential valley occurred at the beginning of every pulse with the valley depth decreasing in successive pulses (curve b in Fig. 7). If the

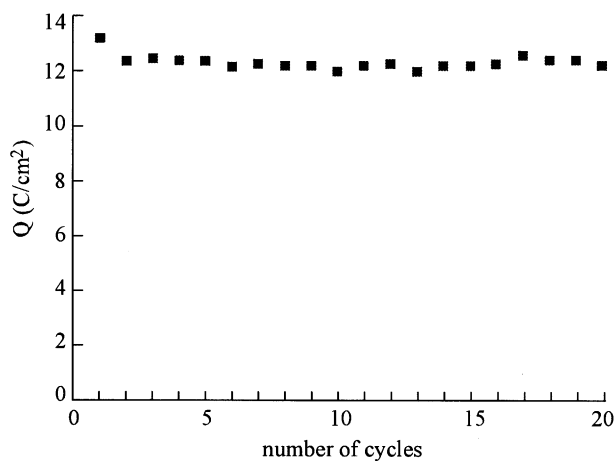


Fig. 6. Variance of discharge capacity with cycling number: 60 and  $400 \text{ mA/cm}^2$  for charge and discharge, respectively. Discharge temperature  $25^\circ\text{C}$ .

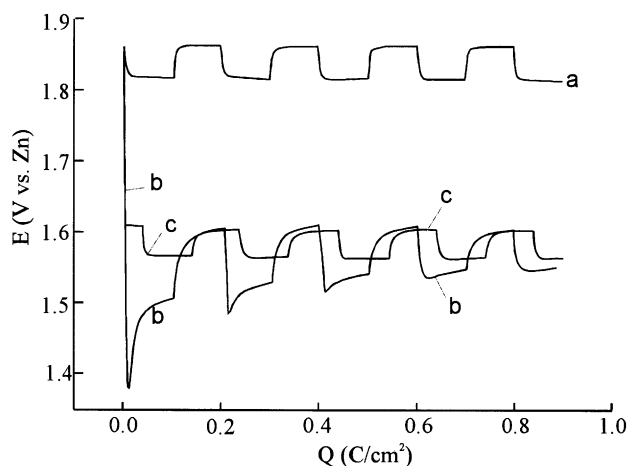


Fig. 7. Pulse discharge immediately after charging: (a) discharge in the high potential regions and (b) low potential regions for a fully charged (to gas evolution) electrode; (c) discharge of an electrode charged to  $4 \text{ C/cm}^2$ . Current pulse amplitude  $0.4 \text{ A/cm}^2$ , pulse width 0.1 s, interval 0.1 s. Discharge temperature  $25^\circ\text{C}$ .

electrode was charged with only a part of the total charge for the low plateau region, for example  $4 \text{ C/cm}^2$ , the potential response was also normal (curve c in Fig. 7). A comparison of curves b and c in Fig. 7 reveals that in the low potential plateau region the electrode charged with only  $4 \text{ C/cm}^2$  performed obviously better than the fully charged one in terms of polarization.

Fig. 8 shows the pulse discharge performance for electrodes which had been on shelf for 20 h in dry state after charge. It is seen by comparing Fig. 8 with Fig. 7 that the short shelf had brought about dramatic changes to the fully charged electrode but not to the one charged only with  $4 \text{ C/cm}^2$ . For the fully charged electrode, the potential of the first pulse dropped down to 1.3 V at the beginning and leveled off well below 1.6 V (curve a in Fig. 8). In other words, the so-called

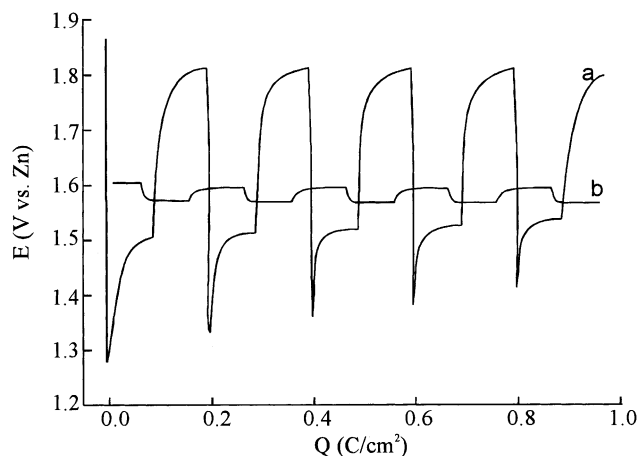


Fig. 8. Pulse discharge after 20 h on shelf in dry charged state: (a) discharge in the high potential regions for a fully charged (to gas evolution) electrode; (b) discharge of an electrode charged to  $4 \text{ C/cm}^2$ . Other conditions are the same as in Fig. 7.

high plateau was only seen during intervals but not during pulses in this case. Besides, there was a deep potential valley for every pulse though the situation improved somewhat with increasing number of pulses. When the open circuit potential decreased to below 1.7 V, the performance was similar to curve b in Fig. 7 and is not shown in Fig. 8. The potential response of the partially charged electrode was not affected by the dry shelf (curve b in Fig. 8).

The above data show that the ultra-thin silver electrode is capable of high rate discharge both in steady-state and in pulses. When a 50  $\mu\text{m}$  silver foil is used as the raw material, after an active layer of 14  $\text{C}/\text{cm}^2$  (for AgO) being developed on each side, the total thickness of the electrode is about 80  $\mu\text{m}$ . The volumetric capacity for the fully charged electrode comes out to be 0.972  $\text{Ah}/\text{cm}^3$  or 972  $\text{Ah}/\text{l}$  while the polarization is about 0.05 V at a volumetric current density 100  $\text{A}/\text{cm}^3$ . The total thickness of the finished electrode may be reduced if a thinner foil is used for the raw material. According to the above described method of electrode preparation, 1  $\text{C}/\text{cm}^2$  capacity (for  $n = 2$ ) corresponds to 1.5  $\mu\text{m}$  thickness of the porous active layer. In electrode design, the thickness of active layer can be estimated based on these parameters and the required capacity. The inner part (solid silver) of the foil serves as the support to the active material and the electrical collector. The thickness of the inner layer should be determined according to the demand on mechanical strength for the support and the conductance for the electrical collector.

The discharge performance of the ultra-thin silver electrode is largely influenced by two main features common to silver oxide electrodes, i.e. the two step reactions and the potential valleys (or peaks) at certain point during discharge (or charge). There have been numerous works to study the reaction mechanisms and the reasons for the potential valleys [13–16]. Some researchers tried to modify the active material so that it contains mainly AgO but discharge at a single (the low) potential plateau [2,17] while others tried to depress the potential valley [18]. Though a few reported approaches seemed effective in the particular cases, they are unlikely suitable to our case. The potential valley is particularly annoying to pulse batteries. A detailed study of this problem is currently in progress in our group and will be reported elsewhere. From the practical point of view, it is suggested based on this work that the ultra-thin silver electrode should be charged with an amount of electricity less than that needed for full conversion of Ag to  $\text{Ag}_2\text{O}$  for the active layer.

#### 4. Summary

Ultra-thin porous silver electrodes for high power pulse batteries are prepared by electrochemical oxidation and reduction of silver foils in HCl solutions. The active layer consists of particles with an average diameter about 0.1  $\mu\text{m}$  after electrochemical activation. The charged ultra-thin silver electrode is capable of discharge at rate over 300C in pulse version. Special attention is paid to the potential valley observed at the beginning of steady-state discharge and the beginning of each current pulse in pulse discharge. For satisfactory potential-valley-free performance, the electrode is suggested to be charged less than the full conversion of Ag to  $\text{Ag}_2\text{O}$  for the active material.

#### Acknowledgements

This work was supported in part by the National Natural Science Foundation of China (Project No. 20073223).

#### References

- [1] A.P. Karpinski, B. Makovetski, S.J. Russell, J.R. Serenyi, D.C. Williams, *J. Power Sources* 80 (1999) 53–60.
- [2] K. Takeda, T. Hattori, *J. Electrochem. Soc.* 146 (1999) 3190.
- [3] J.W. Schultze, M.M. Lohrengel, D. Ross, *Electrochim. Acta* 28 (1983) 363.
- [4] V.I. Birss, C.K. Smith, *Electrochim. Acta* 32 (1987) 259.
- [5] S. Jaya, T.P. Rao, G.P. Rao, *J. Appl. Electrochem.* 17 (1987) 635.
- [6] T. Katan, S. Szpak, D.N. Bennion, *J. Electrochem. Soc.* 120 (1973) 883.
- [7] T.R. Beck, D.E. Rice, *J. Electrochem. Soc.* 131 (1984) 89–93.
- [8] G.D. Nagy, E.J. Casey, in: A. Fleischer, J.J. Lander (Eds.), *Zinc–Silver Oxide Batteries*, Wiley, New York, 1971, p. 133.
- [9] B.D. Cahan, J.B. Ockerman, R.F. Amlie, P. Rüetschi, *J. Electrochem. Soc.* 107 (1960) 725.
- [10] T.P. Dirkse, G.J. Werkema, *J. Electrochem. Soc.* 106 (1959) 88.
- [11] T.P. Dirkse, *J. Electrochem. Soc.* 107 (1960) 859.
- [12] E. Yablokova, E.V. Udalova, G.Z. Kazakevich, *Russ. J. Electrochem.* 31 (1995) 385.
- [13] C.P. Wales, *J. Electrochem. Soc.* 108 (1961) 395.
- [14] C.P. Wales, J. Burbank, *J. Electrochem. Soc.* 112 (1965) 13.
- [15] R.C. Salarezza, J.G. Becerra, A.J. Arvia, *Electrochim. Acta* 33 (1988) 1753.
- [16] T.P. Dirkse, *Electrochim. Acta* 36 (1991) 1533.
- [17] J. Turner, *J. Appl. Electrochem.* 7 (1977) 369.
- [18] V.S. Bagotzky, I.E. Yablokova, G.Z. Kazakevich, T.A. Safronova, in: A.J. Salkind, F.R. McLarnon, S. Bagotzky (Eds.), *The Electrochemistry Society Proceedings on Rechargeable Zinc Batteries*, Series PV 95-14, Pennington, 1995, p. 58.